Conformational properties of an artificial GM1 glycan cluster based on a metal-ligand complex

Yuhei Tachi, Yuko Okamoto, and Hisashi Okumura

Citation: J. Chem. Phys. **149**, 135101 (2018); doi: 10.1063/1.5045310
View online: https://doi.org/10.1063/1.5045310
View Table of Contents: http://aip.scitation.org/toc/jcp/149/13
Published by the American Institute of Physics

Conformational properties of an artificial GM1 glycan cluster based on a metal-ligand complex

Yuhei Tachi,[1,2] Yuko Okamoto,[3,4,5,6] and Hisashi Okumura[2,7,8,a)]
[1]*Department of Physics, Graduate school of Science, Nagoya University, Nagoya, Aichi 464-8602, Japan*
[2]*Research Center for Computational Science, Institute for Molecular Science, Okazaki, Aichi 444-8585, Japan*
[3]*Structural Biology Research Center, Graduate School of Science, Nagoya University, Nagoya, Aichi 464-8602, Japan*
[4]*Center for Computational Science, Graduate School of Engineering, Nagoya University, Nagoya, Aichi 464-8603, Japan*
[5]*Information Technology Center, Nagoya University, Nagoya, Aichi 464-8601, Japan*
[6]*JST-CREST, Nagoya, Aichi 464-8602, Japan*
[7]*Department of Structural Molecular Science, The Graduate University for Advanced Studies, Okazaki, Aichi 444-8585, Japan*
[8]*Exploratory Research Center on Life and Living Systems, National Institutes of Natural Sciences, Okazaki, Aichi 444-8787, Japan*

(Received 19 June 2018; accepted 10 September 2018; published online 1 October 2018)

An artificial glycan cluster, in which 24 monosialotetrahexosylganglioside (GM1) glycans are transplanted to the interface of a metal-ligand complex, was recently proposed to investigate the interaction between GM1 glycan clusters and amyloidogenic proteins by NMR analysis. In this study, all-atom molecular dynamics simulations were performed to characterize the conformational properties of the artificial GM1 glycan cluster. We found that more than 65% of GM1 glycans are clustered by interchain hydrogen bonds. Interchain hydrogen bonds are mainly formed between Neu5Ac and Gal'. Pentamers were most frequently observed in the metal-ligand complex. GM1 glycans are tilted and hydrophobically interact with ligand moieties. The hydrophobic surface of the metal-ligand complex increases intrachain hydrogen bonds in each conformation of the GM1 glycans. The increase of intrachain hydrogen bonds stabilizes the local minimum conformations of the GM1 glycan in comparison with the monomeric one. Interchain hydrogen bonding between glycans and glycan-ligand hydrophobic interactions also contribute to this conformational stabilization. Our results provide the physicochemical properties of the new artificial GM1 glycan cluster under the thermal fluctuations for understanding its protein recognition and designing the drug material for amyloidogenic proteins. *Published by AIP Publishing.* https://doi.org/10.1063/1.5045310

I. INTRODUCTION

Lipid rafts involving monosialotetrahexosylganglioside (GM1) on neuroral cell surfaces mediate cell signaling and immune responses and are involved in the onset and development of various diseases.[1] GM1 is one of the major glycosphingolipids of neuronal cell membranes. GM1 has pentasaccharide structures designated as G1 of ganglio series, and its glycan structure contains a monosialic acid which reflects to the second letter M. GM1 clusters play pathological roles in neurodegenerative diseases caused by the toxic aggregation of proteins such as amyloid-β (Aβ),[2–5] α-synuclein,[6] and prion protein.[7] In the case of Aβ, GM1 clusters specifically interact with Aβ and trigger its structural changes responsible for their aggregation.[8–10] Hence, understanding of these molecular processes has potential importance from the viewpoints of drug development and treatment.[11] To characterize their molecular mechanisms, several artificial GM1 clusters have been proposed, which is mainly analyzed by NMR.[6,12–16] These studies showed that the hydrophobic/hydrophilic environment provided by GM1 clusters induces the α-helix formation of Aβ peptides in multiple steps.[12,13] Previous studies in larger membrane environments revealed that the hydrophobic interior of lipid hydrocarbon chains promotes the α-helix formation of α-synuclein.[17–20]

Recently, a well-defined artificial GM1 glycan cluster, in which 24 GM1 glycan is transplanted to the interface of an $M_{12}L_{24}$ spherical complex,[21,22] has been developed to analyze the early stage of the interaction between GM1 clusters and proteins.[23] The $M_{12}L_{24}$ assembled from 12 palladium ions (M) and 24 bidentate ligands (L) provides a stable scaffold.[24] Artificial GM1 clusters without hydrocarbon chains enabled the NMR spectroscopic characterization of the early stage of its protein recognition. The previous research revealed the recognition site of amyloidogenic proteins Aβ and α-synuclein in the early stage, which was not observed by any previous artificial GM1 clusters.[23] As the recent application, the hyper-self-assembly of $M_{12}L_{24}$ transplanted with 24 Lewis X trisaccharide[25] was also reported. Lewis X clusters mediate cell-cell interactions on cell surfaces.[26–30] The artificial GM1 glycan cluster is expected not only for a novel analytical tool but also for drug discovery and therapy by adsorbing and removing pathogenic substances *in vivo*. Therefore, the

a)Author to whom correspondence should be addressed: hokumura@ims.ac.jp.

properties of the artificial GM1 glycan cluster are important for understanding these biomolecular recognition and logical designing of drug materials. However, despite its importance, the conformational information of the GM1 glycan cluster remains unclear. The difficulty of the experimental direct visualization motivates the necessity of molecular simulations at the atomic level.

Previous molecular dynamics (MD) simulations revealed the properties of GM1 clusters in several membranes.[31–33] Mori *et al.* compared GM1/SM/Chol and GM1/POPC bilayers.[31] Patel *et al.* investigated the influence of GM1 concentration on lipid clustering, the physicochemical properties of membranes, and membrane curvature.[32] Ingòlfsson *et al.* investigated the dynamic properties of GM1 clusters by a plasma membrane model that consists of 63 kinds of lipid.[33] Zhang *et al.* investigated the conformation of monomeric GM1 glycan in solution by replica-exchange MD (REMD) simulations.[34] Several studies also reported the conformation of monomeric N-glycan in solution by REMD simulations.[35–37] In this article, we first modeled the artificial GM1 glycan cluster and investigated the conformational properties of GM1 glycans on the metal-ligand complex (hereinafter we refer to this as just a complex). In particular, we compared the conformational properties of GM1 glycan on the complex and that of well-studied monomeric GM1 glycan by all-atom MD simulations. This comparison helped the conformational characterization of GM1 glycans on the complex.

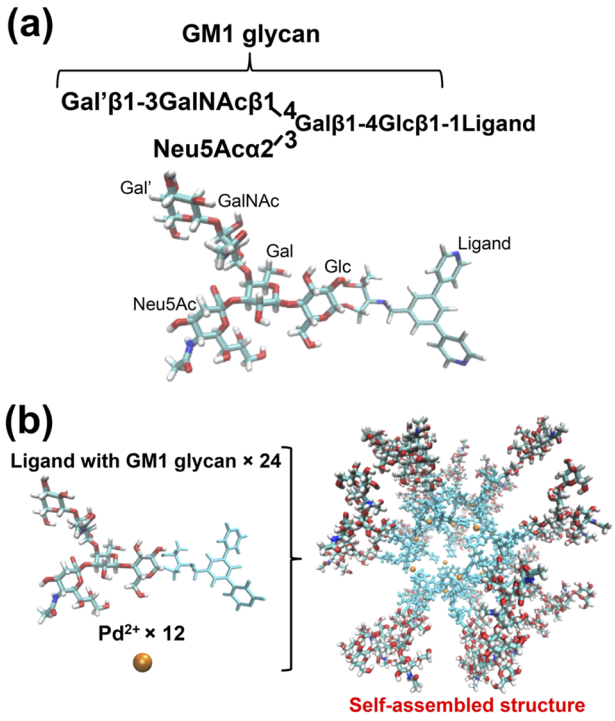

FIG. 1. Molecular structures of the ligand with GM1 glycan and the metal-ligand complex with 24 GM1 glycans used in our simulations. (a) Structure of the ligand with GM1 glycan. In this figure, the Ligand was introduced to connect to GM1 glycans.[23] We refer to a particular ligand as Ligand with a capital L hereafter. (b) Structure of the complex with 24 GM1 glycans.

II. COMPUTATIONAL DETAILS

A. Modeling an artificial GM1 glycan cluster

The artificial GM1 glycan cluster consists of 24 ligands with GM1 pentasaccharide and 12 palladium ions. The configuration of the ligand with GM1 glycan was shown in Fig. 1(a). The self-assembled structure of the artificial GM1 glycan cluster was constructed by placing Ligand parts and palladium ions at the sides and vertices of the cuboctahedral framework of the X-ray crystal structure of the $M_{12}L_{24}$ spherical complex.[21] The configuration of GM1 glycan was constructed by using Glycam Biomolecule Builder.[38] We employed the GLYCAM 06 force field[39] for the GM1 glycan part of the complex and the general AMBER force field (GAFF)[40] for Ligand part. Atomic charge of Ligand part was determined by the restrained electrostatic potential (RESP) charges[41] that were obtained using *ab initio* molecular orbital calculations with the HF/6-31G* level in the Gaussian09 program.[42] To reduce the chances of artifacts caused by trapping in metastable conformations, the charge derivation was performed by splitting Ligand into two parts [see Fig. 2(a)]. The capping of the galactose was employed for structure 1 to take into account the contribution from sugar chain atoms. For the Pd^{2+}-Ligand coordination interactions, the 12-6 Lennard-Jones (LJ) non-bonded model[43] was employed. In Ref. 43, two parameter sets, CM and HFE, are given for the LJ model. We confirmed the stability of the complex by performing 10 ns all-atom molecular dynamics (MD) simulations with both CM and HFE parameter sets. Snapshots after 10 ns simulations are shown in Figs. 2(b) and 2(c). In these figures, we imply that the CM parameter set stabilizes the complex as compared with the HFE parameter set. To reproduce the stability of the complex, we chose the CM parameter set for the 12-6 LJ non-bonded model. Additionally, to observe the glycan conformations on the complex stably, a harmonic restraint with a force constant of 10 kcal/(mol/Å^2) was applied to the Pd^{2+}-N distance. The equilibrium

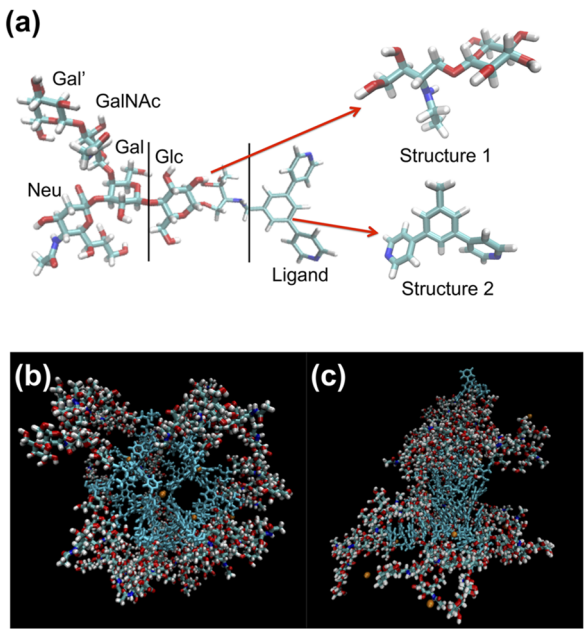

FIG. 2. (a) Two optimized structures splitted from Ligand. Snapshots of the complex with GM1 glycan after 10 ns MD simulation in the case of (b) CM parameter set and (c) HFE parameter set.

distance was set to 2.157 Å. For simplicity, the effect of nitrate (NO^{3-}) counterions of the complex system was ignored in this study.

B. MD simulations

All-atom MD simulations of the complex with 24 GM1 glycans and monomeric GM1 glycan were performed in the *NVT* ensemble for 250 ns using the AMBER16 program package.[44] Temperature was set to 300 K, which was the experimental condition. For conformational sampling, simulations from nine different initial structures were performed on the complex with GM1 glycan, and simulations from 216 different initial structures were performed on the monomeric GM1 glycan. Here, we employed the GLYCAM 06 force field[39] for the glycan part of the complex and the monomeric GM1 glycan, the general AMBER force field (GAFF)[40] for the Ligand part, and the TIP3P model[45] for the water molecules. The complex with GM1 glycan and the monomeric GM1 glycan was solvated with water molecules. The box sizes of the complex with GM1 glycan and the monomeric GM1 glycan were $106 \times 102 \times 102$ Å^3 and $47 \times 44 \times 49$ Å^3, respectively. To neutralize the monomeric system, a hydronium ion was added. All quantities were calculated from the last 150 ns of each simulation. More details are described in the supplementary material.

III. RESULTS AND DISSCUSSION

A typical last 150 ns simulation of the complex is shown in Fig. 3 (Multimedia view). During the simulation, GM1 glycans are not isotropically arranged, but are densely packed on the complex. The exposure of Ligand moiety is also seen in this movie. The exposure of Ligand moiety provides more hydrophobic environment than the sugar chain moiety. Figure 4(a) shows the probability distribution of glycan cluster size (cluster size 1 is a monomer). Here, the glycan cluster was defined as a group connected by hydrogen bonds between the ligands with GM1 glycan. Hydrogen bonds were

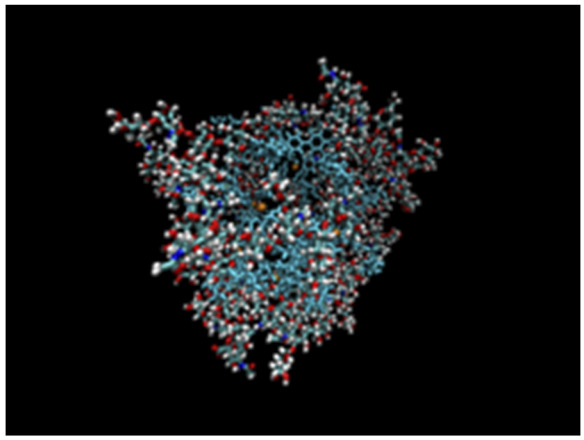

FIG. 3. A movie of a typical last 150 ns simulation trajectory of the complex. Multimedia view: https://doi.org/10.1063/1.5045310.1

determined using the simple geometric criteria: If $R_{AD} < 3.5$ Å and $\theta_{AHD} > 120°$ [R_{AD} is the distance between accepter (A) and donor (D) heavy atoms, and θ_{AHD} is the A–H–D angle] is satisfied, a hydrogen bond was considered to be formed. We found that more than 65% of glycans were clustered on the complex by interchain hydrogen bonding. The cluster size is distributed up to 20. On the complex, pentamers exist with the highest probability. The reason of the highest probability of the pentamers can be explained by the Ligand framework of the complex [see Fig. 4(b)]. The nearest neighbor group of sugar chains on the complex is composed of three sugar chains [red points in Fig. 4(b)] existing on the sides of one triangle. The number of second nearest neighbor sugar chains from the center of the triangle is six [green points in Fig. 4(b)]. However, due to the limitation by the curvature of the spherical complex, only two of the second nearest neighbor sugar chains can bind only two to the nearest neighbor groups. Figure 4(c) shows snapshots of a pentamer during the MD simulation and its Ligand framework. This pentamer was formed as we explained above.

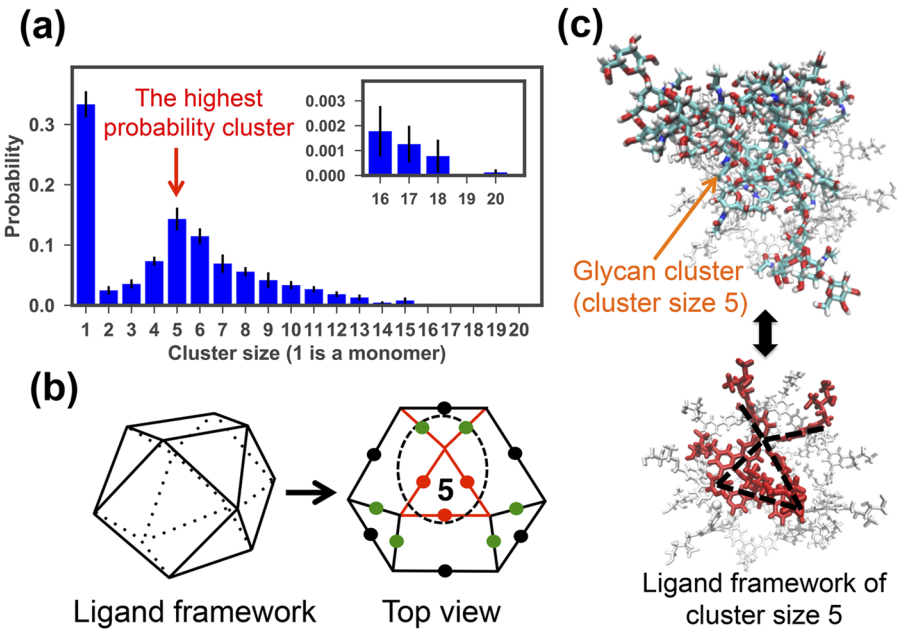

FIG. 4. (a) Probability distribution of glycan cluster size. (b) Cuboctahedral frameworks, in which Ligand moieties correspond to the edges and palladium ions correspond to the vertices. Sugar chain moieties correspond to dots. (c) Snapshots of a GM1 glycan cluster (colored in the upper figure) and its Ligand framework (red in the lower figure) in the case of cluster size 5.

Figure 5(a) shows the probability matrix of interchain hydrogen bond formations among the ligands with GM1 glycan. In this figure, interchain hydrogen bonds are mainly formed between Neu5Ac and Gal'. On the other hand, Gal has low probability overall. Gal is located at the branch point of GM1 glycan. The position of Gal makes it difficult to form a hydrogen bond with the outside of the GM1 glycan. In addition, we calculated the probability matrix of interchain contact formations using different distance cutoffs 3.5 and 5.5 Å [see Figs. 5(b) and 5(c)]. Here, a contact was regarded to be formed between atoms (C, O, N, and Pd^{2+}) located within cutoff distance. The probability matrix of contact formation between palladium ions and sugar molecules was not shown because it was less than 1% of the total contacts. These figures indicate that the sugar chain moiety frequently makes a contact with Ligand moiety. The Ligand has a contact frequently with GalNAc, Neu5Ac, and Gal. The acetyl groups of GalNAc and Neu5Ac interact with Ligand. The hydrophobic surface of Gal and the pyridine ring or benzene ring of Ligand moiety can contact by hydrophobic interactions as previous studies reported that galactose interacts with hydrophobic or aromatic amino acids by its hydrophobic face.[46–48]

The free energy surface with respect to two tilt angles was calculated to investigate the orientation of GM1 glycan on the complex [see Fig. 5(d)]. Radial distribution functions (RDFs) of sugar molecules, Ligands, and water molecules from the center of mass (COM) of Ligands were also calculated (see Fig. S1). This free energy surface and RDFs of sugar molecules and Ligands indicate that GM1 glycans are mainly tilted to the complex side. Note that the peak position of Gal' is the largest in the RDFs. Two tilt angles take on values between 30° and 180° and move flexibly by thermal fluctuations $\sim k_B T$. The C4-C1-COM angle tends to tilt toward the complex compared to the C5-C1-COM angle. This tendency indicates that the Neu side exposes to the solvent compared to the Gal' side because Neu is negatively charged.

To compare the conformational space of GM1 glycan on the complex and the monomeric GM1 glycan, the probability density functions of root-mean-square deviation (RMSD) were calculated [see Fig. 6(a)]. RMSD was calculated by

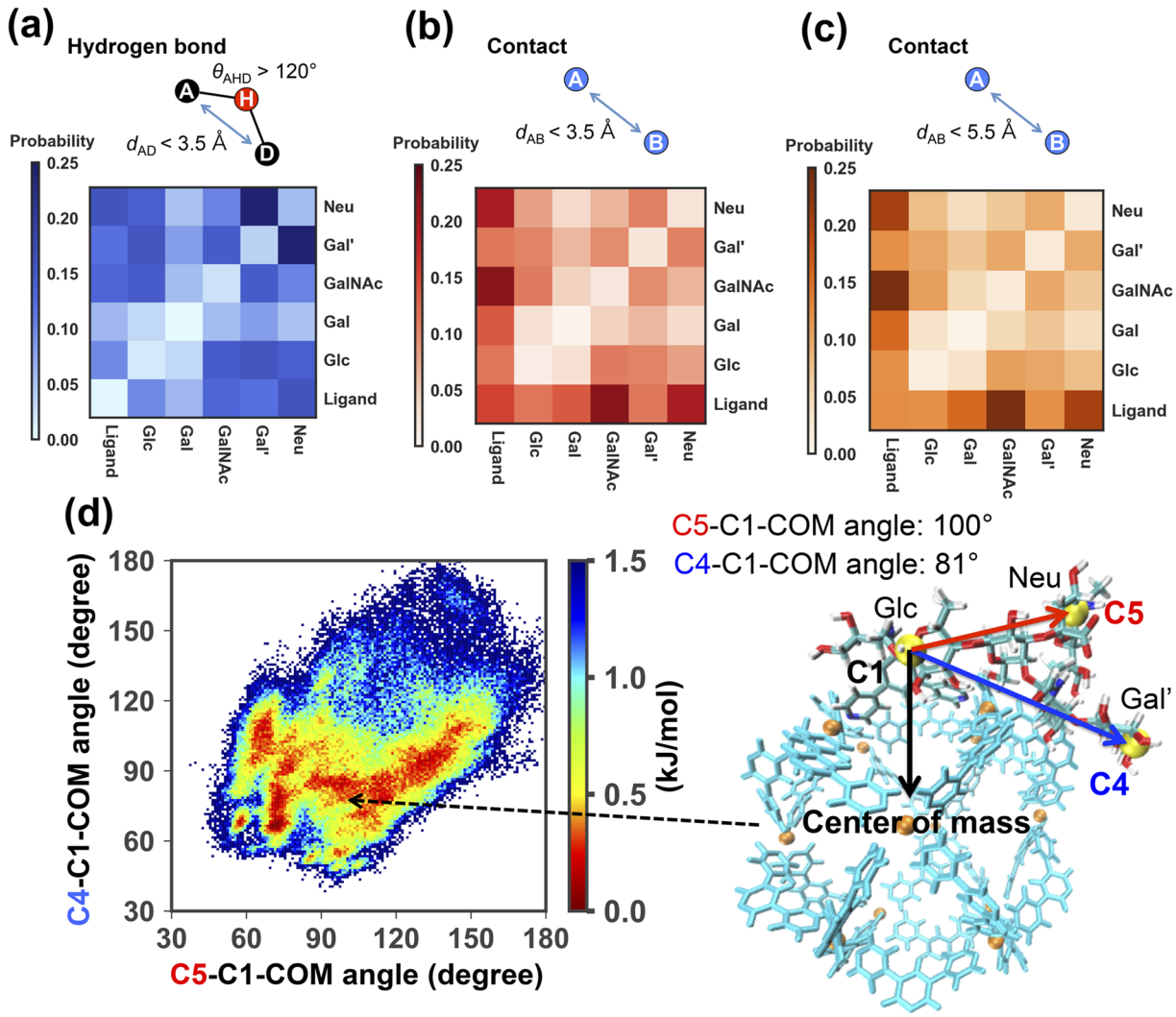

FIG. 5. Probability matrices of interchain interactions among the ligands with GM1 glycan: (a) hydrogen bond formations, (b) contact formations using 3.5 Å cutoff, and (c) contact formations using 5.5 Å cutoff. (d) Free energy surface composed of two tilt angles. The C4-C1-COM angle is the angle between two vectors, which are C1 to C4 vector and C1 to the center of mass (COM) of Ligands vector. The C5-C1-COM angle is the angle between two vectors, which are C1 to C5 vector and C1 to the COM of the Ligand vector.

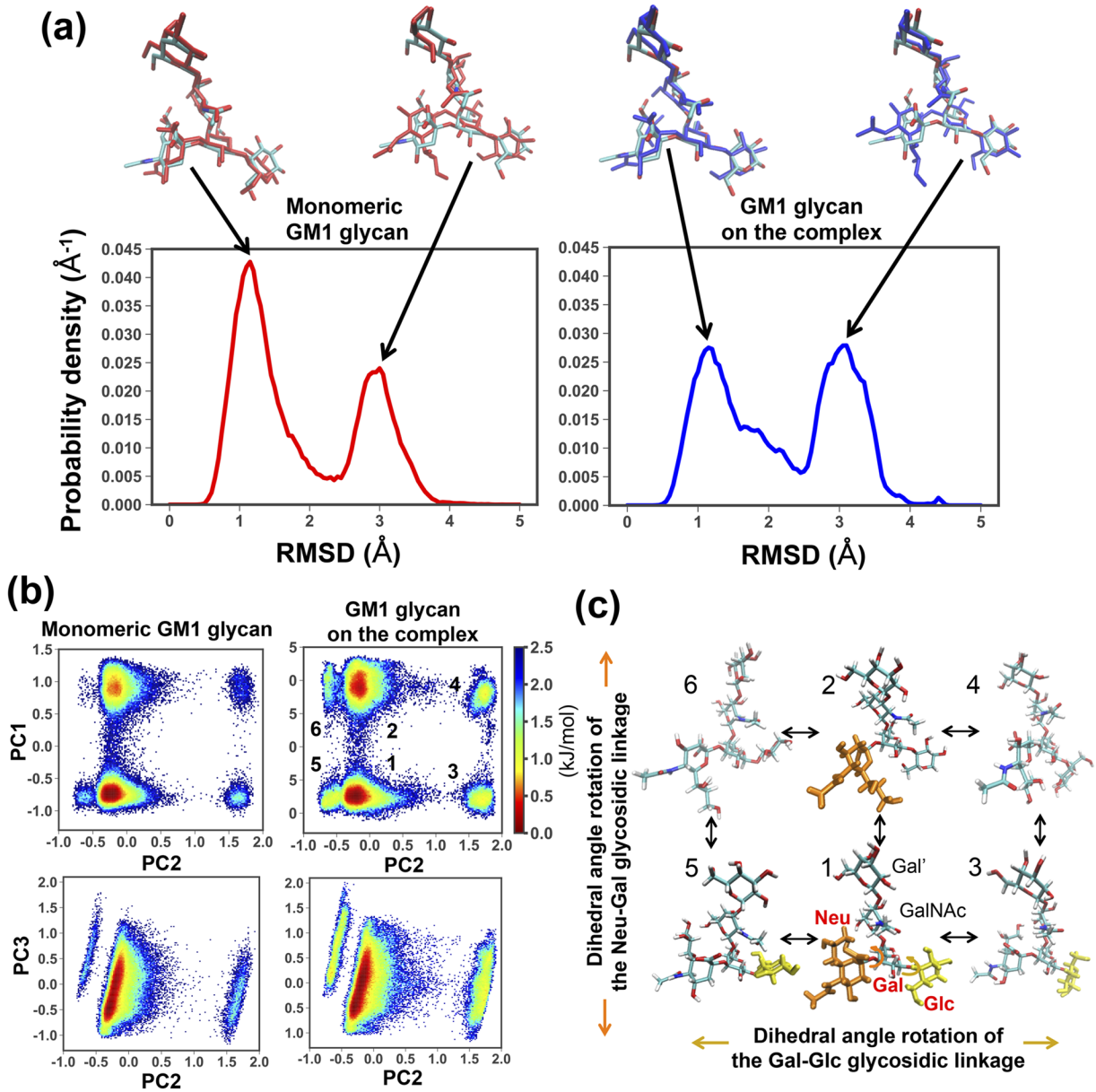

FIG. 6. (a) Probability density functions of root-mean-square deviation (RMSD) with respect to a representative GM1 glycan structure (PDB: 3CHB) of GM1 glycan on the complex and the monomeric GM1 glycan. (b) Free energy surface composed of the first two eigenvectors PC1 and PC2 and the second and the third eigenvectors PC2 and PC3 in each system. (c) The six major conformations in the case of GM1 glycan on the complex.

superposing the GM1 glycan structure of each trajectory on a representative GM1 glycan structure (PDB: 3CHB).[49] The position of the highest peak was the same in both cases. However, in the case of GM1 glycan on the complex, the position of the second highest peak has a slightly larger value and the difference of the probability density value between two peaks is much smaller. Free energy surfaces of dihedral angles (Φ_n, Ψ_n, n = 1, 2, 3, and 4) of four glycosidic linkages were also calculated in each system (see Figs. S2 and S3). In both cases, there is no significant difference in the position of the stable point of these free energy surfaces.

To compare the conformational stability in more detail, dihedral angle principle component analysis (dPCA) analysis was carried out. This method was proposed to describe the rugged free energy landscape of protein folding by using sine/cosine-transformed dihedral angles of a peptide backbone.[50] We employed dihedral angles of the glycosidic linkages, instead of the peptide backbone. Figure 6(b) shows free energy surfaces as a function of the first two eigenvectors PC1 and PC2 and the second and third eigenvectors PC2 and PC3 in each system. We found that the rotation of dihedral angles of the glycosidic linkage of Neu-Gal and Gal-Glc contributes to the PC1 and PC2 by calculating correlation coefficients. From this figure, we found that the GM1 glycan has six major conformations in both cases. In the case of GM1 glycan on the complex, the local minima 3, 4, 5, and 6 are remarkably stabilized compared with the monomeric GM1 glycan. Snapshots of each conformation on the complex are shown [see Fig. 6(c)]. Additionally, we also calculated free energy surfaces as a function of the PC1-PC2 space and the PC2 and

PC3 space in each cluster size, up to 20 (see Figs. S4 and S5). These figures show that major conformations in each cluster size are distributed as the same as that of the entire conformational space on the complex, and conformation 1 or 2 is the most stable state in each glycan cluster.

To clarify the reason for the stabilization of conformation 3, 4, 5, and 6 on the complex, the average number of hydrogen bonds and the free energy surface of the two tilt angles were calculated in each conformation (see Figs. S6 and S7). There are two reasons for the stabilization of the local minima. The first one is explained from the average number of intra- and inter-chain hydrogen bonds of each conformation in the monomeric GM1 glycan and GM1 glycan on the complex (see Fig. S6). Compared to the monomeric case, GM1 glycan on the complex has more intrachain hydrogen bonds. The hydrophobic environment increases the stability of electrostatic interaction because the dielectric constant decreases under the lower densities of water molecules.[51] The RDF of water molecules (see Fig. S1) shows that there are fewer water molecules at the position where the sugar molecules are present ($r \sim 20$ Å). Among the six conformations, the average number of intrachain hydrogen bonds is particularly increased in conformations 5 and 6. Interchain hydrogen bonding also contributes to the stabilization of conformation 6. Because, conformation 6 has more interchain hydrogen bonds than conformation 1. Thus, these conformations are stabilized as compared with the monomeric case by intra- and inter-chain hydrogen bonding. The second one is explained from free energy surfaces of the two tilt angles in each conformation (see Fig. S7). Conformations 3 and 4 have lower tilt angles. The lower tilt angles increase the hydrophobic interaction between the GM1 glycan and Ligand. Therefore, conformation 3 and 4 are stabilized as compared with the monomeric case by sugar-Ligand hydrophobic interactions.

IV. CONCLUSIONS

In this study, we investigated the conformational properties of the new artificial GM1 glycan cluster, which is based on a metal-ligand complex by all-atom MD simulations. Comparison with the simulations of the monomeric GM1 glycan helped us to characterize the GM1 glycan conformations on the metal-ligand complex more clearly. From the analysis of MD trajectories, we found that more than 65% of GM1 glycans were clustered by interchain hydrogen bonding. Interchain hydrogen bonding between Neu5Ac and Gal' was frequently observed on the complex. The glycan cluster with the highest probability was pentamer. On the other hand, there are areas where Ligand moiety is exposed at the interface with water molecules. On the complex, GM1 glycans are mainly tilted and interact with Ligand moieties. Furthermore, the increase of the number of intrachain hydrogen bonds on the hydrophobic surface of the metal-ligand complex stabilizes the local minimum conformations of the GM1 glycan compared to the monomeric GM1 glycan. Interchain hydrogen bonding and glycan-Ligand hydrophobic interactions also contribute to this conformational stabilization. The findings of conformational properties enable us to elucidate the binding mechanism of amyloidogenic proteins to the GM1 glycan cluster. In a future study, we will report the results of further simulations including interactions with amyloidogenic proteins, which will give a physicochemical understanding of the protein recognition mechanism.

SUPPLEMENTARY MATERIAL

See supplementary material for computational details and additional figures.

ACKNOWLEDGMENTS

This work was supported by the JSPS Grant-in-Aid for Scientific Research on Innovative Areas (Grant Nos. JP25102007 and JP16H00790). We used supercomputers at the Research Center for Computational Science, Okazaki Research Facilities, National Institutes of Natural Sciences in Japan and the facilities of the Supercomputer Center, the Institute for Solid State Physics, the University of Tokyo in Japan.

[1] V. Michel and M. Bakovic, Biol. Cell **99**, 129–140 (2007).
[2] Y. Mao, Z. Shang, Y. Imai, T. Hoshino, R. Tero, M. Tanaka, N. Yamamoto, K. Yanagisawa, and T. Urisu, Biochim. Biophys. Acta **1798**, 1090–1099 (2010).
[3] A. Kakio, S. Nishimoto, K. Yanagisawa, Y. Kozutsumi, and K. Matsuzaki, Biochemistry **41**, 7385–7390 (2002).
[4] T. Hoshino, M. I. Mahmood, K. Mori, and K. Matsuzaki, J. Phys. Chem. B **117**, 8085–8094 (2013).
[5] J. Fantini, N. Yahi, and N. Garmy, Front. Physiol. **4**, 120 (2013).
[6] J. Fantini and N. Yahi, J. Mol. Biol. **408**, 654–669 (2011).
[7] L. Botto, D. Cunati, S. Coco, S. Sesana, A. Bulbarelli, E. Biasini, L. Colombo, A. Negro, R. Chiesa, M. Masserini, and P. Palestini, PLoS One **9**, e98344 (2014).
[8] K. Yanagisawa, A. Odaka, N. Suzuki, and Y. Ihara, Nat. Med. **1**, 1062–1066 (1995).
[9] K. Matsuzaki, K. Kato, and K. Yanagisawa, Biochim. Biophys. Acta **1801**, 868–877 (2010).
[10] L.-P. Choo-Smith and W. K. Surewicz, FEBS Lett. **402**, 95–98 (1997).
[11] Y. Kamiya, M. Yagi-Utsumi, H. Yagi, and K. Kato, Curr. Pharm. Des. **17**, 1672–1684 (2011).
[12] M. Yagi-Utsumi, H. Yamaguchi, N. Sasakawa, K. Yamamoto, K. Yanagisawa, and K. Kato, Glycoconjugate J. **26**, 999–1006 (2009).
[13] M. Yagi-Utsumi, T. Kameda, Y. Yamaguchi, and K. Kato, FEBS Lett. **584**, 831–836 (2010).
[14] M. Yagi-Utsumi, K. Matsuo, K. Yanagisawa, K. Gekko, and K. Kato, Int. J. Alzheimers Dis. **2011**, 925073 (2010).
[15] Z. Martinez, M. Zhu, S. Han, and A. L. Fink, Biochemistry **46**, 1868–1877 (2007).
[16] T. Yamaguchi, T. Uno, Y. Uesaka, M. Yagi-Utsumi, and K. Kato, Chem. Commun. **49**, 1235–1237 (2013).
[17] T. S. Ulmer, A. Bax, N. B. Cole, and R. L. Nussbaum, J. Biol. Chem. **280**, 9595–9603 (2005).
[18] C. R. Bodner, C. M. Dobson, and A. Bax, J. Mol. Biol. **390**, 775–790 (2009).
[19] C. R. Bodner, A. S. Maltsev, C. M. Dobson, and A. Bax, Biochemistry **49**, 862–871 (2010).
[20] T. Bartels, L. S. Ahlstrom, A. Leftin, F. Kamp, C. Haass, M. F. Brown, and K. Beyer, Biophys. J. **99**, 2116–2124 (2010).
[21] M. Tominaga, K. Suzuki, M. Kawano, T. Kusukawa, T. Ozeki, S. Sakamoto, K. Yamaguchi, and M. Fujita, Angew. Chem., Int. Ed. **43**, 5621–5625 (2004).
[22] N. Kamiya, M. Tominaga, S. Sato, and M. Fujita, J. Am. Chem. Soc. **129**, 3816–3817 (2007).
[23] S. Sato, Y. Yoshimasa, D. Fujita, M. Yagi-Utsumi, T. Yamaguchi, K. Kato, and M. Fujita, Angew. Chem., Int. Ed. **54**, 8435–8439 (2015).
[24] S. Sato, Y. Ishido, and M. Fujita, J. Am. Chem. Soc. **131**, 6064–6065 (2009).
[25] G. Yan, T. Yamaguchi, T. Suzuki, S. Yanaka, S. Sato, M. Fujita, and K. Kato, Chem. - Asian J. **12**, 968–972 (2017).
[26] N. Kojima, B. A. Fenderson, M. R. Stroud, R. I. Goldberg, R. Habermann, T. Toyokuni, and S. Hakomori, Glycoconjugate J. **11**, 238–248 (1994).

[27]S. Hanashima, K. Kato, and Y. Yamaguchi, Chem. Commun. **47**, 10800–10802 (2011).
[28]A. Geyer, C. Gege, and R. R. Schmidt, Angew.Chem., Int. Ed. **39**, 3245–3249 (2000).
[29]M. J. Hernàiz, J. M. de la Fuente, À. G. Barrientos, and S. Penadès, Angew. Chem. **114**, 1624–1627 (2002).
[30]J. M. de la Fuente, P. Eaton, À. G. Barrientos, M. Menèndez, and S. Penadès, J. Am. Chem. Soc. **127**, 6192–6197 (2005).
[31]K. Mori, M. I. Mahmood, S. Neya, K. Matsuzaki, and T. Hoshino, J. Phys. Chem. B **116**, 5111–5121 (2012).
[32]D. S. Patel, S. Park, E. L. Wu, M. S. Yeom, G. Widmalm, J. B. Klauda, and W. Im, Biophys. J. **111**, 1987–1999 (2016).
[33]H. I. Ingòlfsson, M. N. Melo, F. J. van Eerden, C. Arnarez, C. A. Lopez, T. A. Wassenaar, X. Periole, A. H. de Vries, D. P. Tieleman, and S. J. Marrink, J. Am. Chem. Soc. **136**, 14554–14559 (2014).
[34]Y. Zhang, T. Yamaguchi, T. Satoh, M. Yagi-Utsumi, Y. Kamiya, Y. Sakae, Y. Okamoto, and K. Kato, Adv. Exp. Med. Biol. **842**, 217–230 (2015).
[35]S. Re, N. Miyashita, Y. Yamaguchi, and Y. Sugita, "Structural diversity and changes in conformational equilibria of biantennary complex-type N-glycans in water revealed by replica-exchange molecular dynamics simulation," Biophys. J. **101**, L44–L46 (2011).
[36]W. Nishima, N. Miyashita, Y. Yamaguchi, Y. Sugita, and S. Re, "Effect of bisecting GlcNAc and core fucosylation on conformational properties of biantennary complex-type N-glycans in solution," J. Phys. Chem. B **116**, 8504–8512 (2012).
[37]T. Yamaguchi, Y. Sakae, Y. Zhang, S. Yamamoto, Y. Okamoto, and K. Kato, Angew. Chem., Int. Ed. **53**, 10941–10944 (2014).
[38]Woods Group, GLYCAM Web, Complex Carbohydrate Research Center, University of Georgia, Athens, GA, 2005-2018, http://glycam.org.
[39]K. N. Kirschner, A. B. Yongye, S. M. Tschampel, J. Gonzàlez-Outeiriño, C. R. Daniels, B. L. Foley, and R. J. Woods, J. Comput. Chem. **29**, 622–655 (2008).
[40]J. Wang, R. M. Wolf, R. M. Caldwell, P. A. Kollman, and D. A. Case, J. Comput. Chem. **25**, 1157–1174 (2004).
[41]C. I. Bayly, P. Cieplak, W. Cornell, and P. A. Kollman, J. Chem. Phys. **97**, 10269–10280 (1993).
[42]M. J. Frisch, G. W. Trucks, H. B. Schlegel, G. E. Scuseria, M. A. Robb, J. R. Cheeseman, G. Scalmani, V. Barone, B. Mennucci, G. A. Petersson, H. Nakatsuji, M. Caricato, X. Li, H. P. Hratchian, A. F. Izmaylov, J. Bloino, G. Zheng, J. L. Sonnenberg, M. Hada, M. Ehara, K. Toyota, R. Fukuda, J. Hasegawa, M. Ishida, T. Nakajima, Y. Honda, O. Kitao, H. Nakai, T. Vreven, J. A. Montgomery, Jr., J. E. Peralta, F. Ogliaro, M. Bearpark, J. J. Heyd, E. Brothers, K. N. Kudin, V. N. Staroverov, R. Kobayashi, J. Normand, K. Raghavachari, A. Rendell, J. C. Burant, S. S. Iyengar, J. Tomasi, M. Cossi, N. Rega, J. M. Millam, M. Klene, J. E. Knox, J. B. Cross, V. Bakken, C. Adamo, J. Jaramillo, R. Gomperts, R. E. Stratmann, O. Yazyev, A. J. Austin, R. Cammi, C. Pomelli, J. W. Ochterski, R. L. Martin, K. Morokuma, V. G. Zakrzewski, G. A. Voth, P. Salvador, J. J. Dannenberg, S. Dapprich, A. D. Daniels, Ö. Farkas, J. B. Foresman, J. V. Ortiz, J. Cioslowski, and D. J. Fox, GAUSSIAN 09, Revision D.01, Gaussian, Inc., Wallingford, CT, 2009.
[43]P. Li, B. P. Roberts, D. K. Chakravorty, and K. M. Merz, Jr., J. Chem. Theory Comput. **10**, 289–297 (2014).
[44]D. A. Case, R. M. Betz, D. S. Cerutti, T. E. Cheatham III, T. A. Darden, R. E. Duke, T. J. Giese, H. Gohlke, A. W. Goetz, N. Homeyer, S. Izadi, P. Janowski, J. Kaus, A. Kovalenko, T. S. Lee, S. LeGrand, P. Li, C. Lin, T. Luchko, R. Luo, B. Madej, D. Mermelstein, K. M. Merz, G. Monard, H. Nguyen, H. T. Nguyen, I. Omelyan, A. Onufriev, D. R. Roe, A. Roitberg, C. Sagui, C. L. Simmerling, W. M. Botello-Smith, J. Swails, R. C. Walker, J. Wang, R. M. Wolf, X. Wu, L. Xiao, and P. A. Kollman, *AMBER 2016* (University of California, San Francisco, 2016).
[45]W. L. Jorgensen, J. Chandrasekhar, J. D. Madura, R. W. Impey, and M. L. Klein, J. Chem. Phys. **79**, 926–935 (1983).
[46]M. S. Sujatha and P. V. Balaji, Proteins **55**, 44–65 (2004).
[47]M. S. Sujatha, Y. Sasidhar, and P. Balaji, Biochemistry **44**, 8554–8562 (2005).
[48]C. Chen, S. Song, N. Gilboa-Garber, K. Chang, and A. Wu, Glycobiology **8**, 7–16 (1998).
[49]E. A. Merritt, P. Kuhn, S. Sarfaty, J. L. Erbe, R. K. Holmes, and W. G. Hol, J. Mol. Biol. **282**, 1043–1059 (1998).
[50]Y. Mu, P. H. Nguyen, and G. Stock, Proteins **58**, 45–52 (2005).
[51]N. Yoshii, S. Miura, and S. Okazaki, Chem. Phys. Lett. **345**, 195–200 (2001).